

# Improved STATCOM Operation Under Transient Disturbances for Wind Power Applications

Ion Etxeberria-Otadui<sup>(1)</sup>, Unai Viscarret<sup>(1)</sup>, Izaskun Zamakona<sup>(2)</sup>, Beatriz Arenal Redondo<sup>(3)</sup>,  
Javier Ibiricu<sup>(4)</sup>

<sup>(1)</sup> IKERLAN-IK4 Technology Research Centre, Apdo. 146, E-20.500 Mondragón (Spain)  
Tel: +34 943 712400, FAX: +34 943796944, [ietxeberria@ikerlan.es](mailto:ietxeberria@ikerlan.es), [uviscarret@ikerlan.es](mailto:uviscarret@ikerlan.es)

<sup>(2)</sup> OLDAR Electrónica, S.A., Barrio Basauntz, 2, E-48140 Igorre (Spain)  
Tel: +34 946 305 113, Fax: + 34 946 305 112, [izc@oldar-electronica.com](mailto:izc@oldar-electronica.com)

<sup>(3)</sup> JEMA, Paseo del Circuito nº10, E-20160 Lasarte-Oria (Spain)  
Tel: +34 943 37 64 00, Fax: +34 943 37 12 79, [b.arenal@grupojema.com](mailto:b.arenal@grupojema.com)

<sup>(4)</sup> Eólicas de Euskadi, Parque Tecnológico de Álava, E-6, oficina 309, 01510, Miñano (Spain)  
Tel: +34 945 29 69 45, Fax: 945 29 69 46, [jibiricu@eolicaseuskadi.com](mailto:jibiricu@eolicaseuskadi.com)

## Acknowledgements

This work was supported in part by the Basque Regional Government in the context of the Project SICRE: *Sistema de Inyección de Corriente Reactiva para Instalaciones de Producción Eléctrica en Régimen Especial*.

## Keywords

STATCOM, Converter Control, Wind Energy.

## Abstract

This paper presents an optimized STATCOM control for wind power applications. The transient behavior of fixed-speed wind farms can be improved by injecting large amounts of reactive power during the fault recovery. This application requires a high dynamic converter, which must also be capable of working under transient unbalanced conditions. Here, a stationary control structure is proposed, which is based on resonant regulators and a DFT synchronization algorithm, which allows an optimized reactive power injection during voltage dips occurred in the grid. The proposed structure is validated experimentally using a reduced scale STATCOM prototype, showing that it is well adapted for the concerned application.

## 1. Introduction: STATCOMs in wind power applications

The vision of the contribution of Static VAR Compensation devices in wind power applications has evolved in the last few years. Initially, at the end of the 1990s, it was assumed that their main function was wind power quality improvement, i.e., fixing a unity output power factor and thus reducing voltage drops, flicker, and electrical losses in the network during normal operation [1]. An example of this viewpoint is the 8 MVar experimental STATCOM that was installed in 1998 in the Rejsby Hede (Denmark) wind farm [2] in the context of a European Commission funded project [3]. Later on, with the development and expansion of doubly fed induction generators and the generalized practice of connecting the wind farms in sufficiently strong networks, the interest of using Static VAR Compensation devices in wind farms has been flagging. However, with the publication of new and more restrictive interconnection requirements they are currently drawing increasing interest [4], [5], [6], [7], [8]. Until recently wind farms were required to disconnect from the grid in case of disturbance, losing therefore their generation capability at a critical moment for the system operation.

Consequently, newly developed Grid-Codes [9] request them a *Low Voltage Ride Through* (LVRT) capability: they must be able to withstand without disconnection voltage disturbances above a certain limit characteristic (defined in terms of depth and duration) as shown in Figure 1.

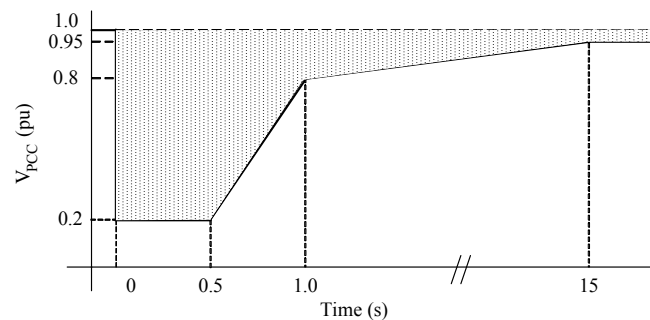


Fig. 1. Fault ride-through characteristic specified by the Spanish grid operator [9].

STATCOMs can be employed to improve fixed-speed wind farm behavior during the most critical phase of a grid-disturbance, the voltage recovery after the clearing, by injecting the reactive power required by the generators and avoiding this way the voltage drop provoked by the absorption of this power from the grid. Let us analyze in detail the fault behavior of fixed-speed wind farms.

Voltage dips have a double effect on fixed-speed wind turbines: electrical and mechanical. The main electrical effect is the demagnetization of the rotor while the most significant mechanical one is the rotor speed increase [10]. These effects are observable from the beginning of the dip until a few seconds after its recovery (see Fig. 2, where a 0.2 p.u. 3 phase sag is applied to a 36 MW fixed-speed wind farm from  $t = 0.5$ s to  $t = 0.6$ s using PSCAD/EMTDC). The terminal voltage dip provokes the demagnetization of the stator flux. However, the rotor flux cannot decrease instantaneously and therefore the machine current goes through a hard transient (it may reach several p.u.) in which it delivers reactive power to the network.

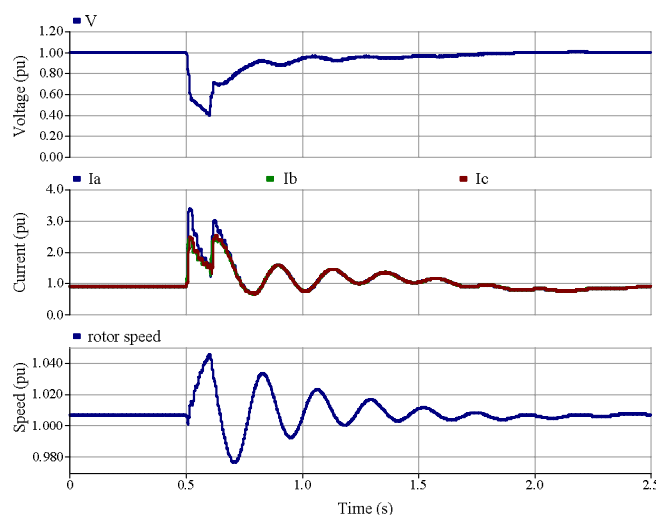


Fig. 2. Terminal voltage, stator RMS current and rotor speed of a fixed-speed wind turbine after a 0.1 s short-circuit.

In addition, the active power exported to the grid is significantly reduced during the fault while the input mechanical power from the wind turbine is almost constant (the wind speed can be considered to be unvaried and the mechanical power limitation systems require a non negligible time -pitch control- or rotational speed increase -stall control- to react). Therefore the generator will accelerate during the short-circuit in order to mechanically store the energy excess. The achieved speed must be lower than the maximum tolerable speed to avoid the disconnection of the generator.

After the clearing, the generator consumes large amounts of reactive power due to its magnetization and to the increase of the machine slip during the fault. This power consumption makes it difficult the recovery of the terminal voltage. If the voltage does not recover fast enough, the machine will continue accelerating until its final disconnection.

The best way to avoid voltage dip derived problems on wind generators is to control the connection point voltage by compensating voltage dips and protecting the facility from any voltage imperfection. This can be done by using a series power electronic compensator *Dynamic Voltage Restorer* (DVR) which injects the necessary voltage in the system in order to keep the generator voltage constant [11]. However, this compensator requires an active power absorption capability during faults (in order to deal with the power generated by the wind farm that can not be exported to the grid) which its main drawback. If a shunt compensator (SVC or STATCOM) is used, little can be done during the fault in order to improve the voltage due to the huge amount of power that would be necessary. Nevertheless, the shunt compensator can be used to improve the behavior of the system after the clearing of the fault avoiding the voltage drop provoked by the absorption of this power from the grid. This is the most widely proposed compensator-based solution for the ride-through capability improvement of fixed-speed wind turbines [4], [5].

However, as the STATCOM will have to be operated during unbalanced faults it will have to be designed for this kind of operation, optimizing the reactive power injected into the grid at any condition. Therefore the main scope of the paper is to propose an improved control structure in order to optimize STATCOM operation under transient disturbances for wind power applications

## 2. STATCOM operation under unbalanced transient disturbances

In this section the operation of a generic vector current controlled PWM converter (see Figure 3) will be analyzed under unbalanced transient conditions. The controller includes a negligible dynamics PLL (it does not react during transient disturbances) in order to reject harmonic and negative sequence phase disturbances. In addition, it is considered that the converter is not affected by zero-sequence voltage disturbances because of the presence of zero-sequence blocking transformers [12].

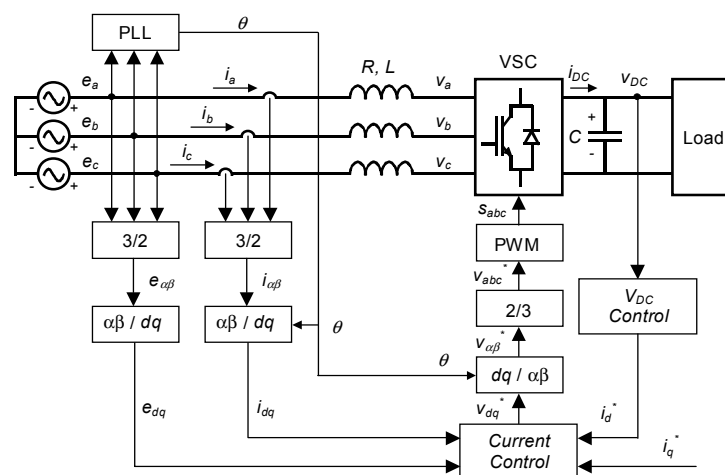


Fig. 3. Generic Single Reference Frame Vector Current Controller.

The first and immediate effect of a voltage dip is the decrease of the exchanged power and also of the maximum exchangeable power. In general the converter controller will try to keep the exchanged power constant and therefore current amplitude will increase. In addition, phase angle shifts ( $\Delta\theta$ ) provoke a synchronization error during faults (due to the negligible PLL dynamics). This error may have a different impact on the operation depending on the considered application.

Let us analyze 2 possible grid-connected applications: a rectifier (PF = 1) and a STATCOM (PF = 0).

- Rectifier (PF = 1): synchronization errors results in an undesired reactive component,  $I_{dq}$ , as well as a decrease of the active current,  $I_{dd}$ ,

$$\begin{aligned} I_{dq} &= I'_d \cdot \sin(\Delta\theta) \\ I_{dd} &= I'_d \cdot \cos(\Delta\theta) \end{aligned} \tag{1}$$

where  $I'_d$  is the desired active current (see Fig. 4 left, where  $dq$  is the real synchronous reference frame and  $dq'$  is the estimated one). Therefore, there will be a power factor error:

$$\Delta PF = 1 - \cos(\Delta\theta) \tag{2}$$

If the system contains a power feedback loop (measured phase per phase) exchanged power error can be detected and used for phase angle jump estimation, minimizing the error in fault steady-state.

- STATCOM (PF = 0): synchronization errors results in an undesired active component:

$$I_{qd} = I'_q \cdot \sin(\Delta\theta) \tag{3}$$

where  $I'_q$  is the desired reactive current (see Fig. 4 right, where  $dq$  is the real synchronous reference frame and  $dq'$  is the estimated one).

However, as the converter has no active power exchange capability (other than for power losses compensation purposes) the bus voltage controller will react modifying the “active” current reference ( $I'_d$ ) until its real active projection ( $I_{dd}$ ) compensates the erroneously injected active current ( $I_{qd}$ ).

$$\Delta I_q = I'_q - I_{qq} - I_{dq} = \frac{1 - \cos \Delta\theta}{\cos \Delta\theta} \tag{4}$$

This error increases very rapidly with the phase angle shift value, reaching a considerable value (100% increase) for the maximum considered jump ( $60^\circ$ ) [12]. In this case the error can also be minimized during the time between the voltage dip beginning and end using the exchanged power error.

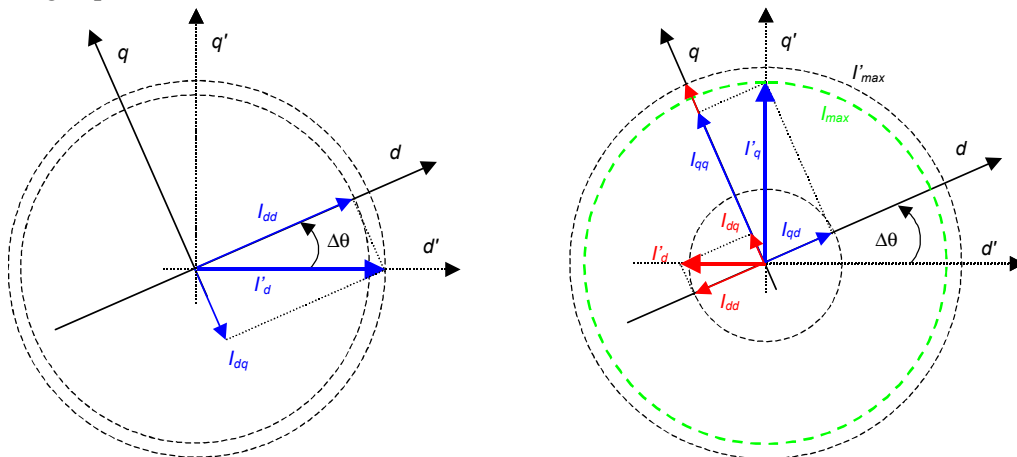


Fig. 4. Impact of a phase angle jump on a rectifier (left) and a STATCOM (right) operation.

Besides the converter current, DC bus voltage may also be distorted during disturbances. In case of a balanced voltage dip, DC bus voltage transients can be observed both at the beginning and at the end of the disturbance, but there are no steady-state oscillations during the disturbance due to the power balance between phases.

The case of unbalanced voltage dips is different. They are characterized by a decrease of the positive voltage sequence and the appearance of a negative voltage sequence. Thus, generally a power unbalance will take place between phases, which will lead to double grid frequency oscillations in the DC bus (in addition to fault beginning and end transients). In addition, there may also be a phase angle

unbalance between difference phases. However, and supposing that there is a zero-sequence blocking transformer between the fault origin and the converter, there will always be some kind of symmetry between phases. As a result, undesired power components due to phase angle unbalances are compensated between phases and do not affect DC bus voltage. Figure 5 shows this compensation phenomenon for a pure reactive operation mode and 2 different voltage sags ( $I_{bd} = -I_{cd}$ ).

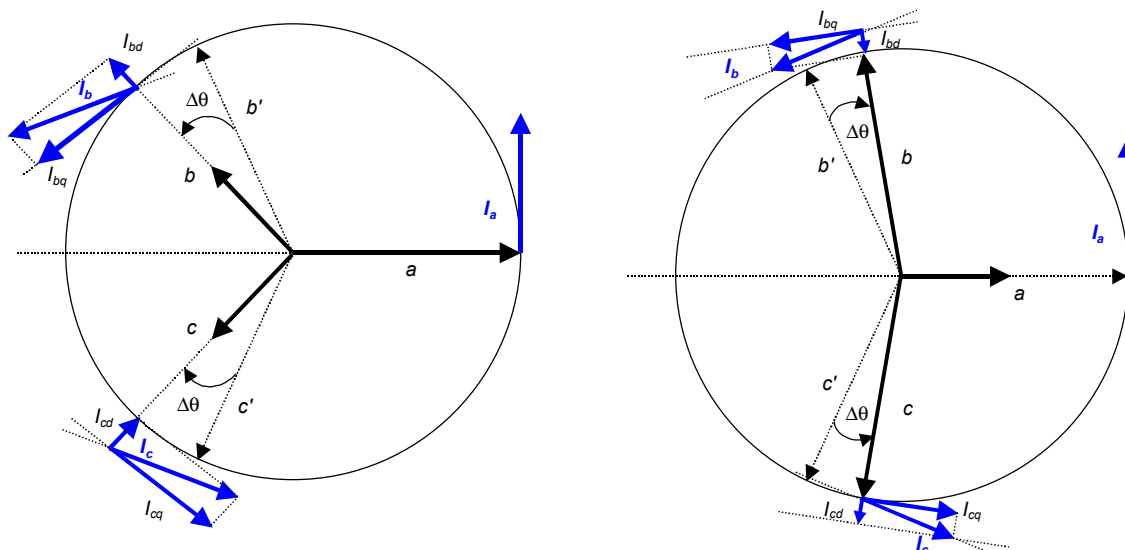


Fig. 5. Compensation of undesired current components in unbalanced voltage sags (pure reactive operation and 2 different voltage sags).

In addition, depending on the implemented controller, converter current may also be distorted and unbalanced. The main cause of current distortion is the DC bus voltage harmonic propagation through the current reference generated by the DC bus voltage loop, and therefore it can be easily avoided by filtering this reference. Concerning current unbalances, they are originated by the incapacity of the control to completely reject negative current sequence disturbances, and therefore they can be avoided by improving this controller feature. Summarizing, the main effects of transient voltage dips on the operation of power converters are or maybe:

1. Decrease of the maximum power exchange between the converter and the grid.
2. Power factor and/or current amplitude error (in case of phase angle jump).
3. DC bus voltage oscillations (at the beginning and at the end of the disturbance as well as stationary oscillations in case of power unbalance).
4. Unbalance and distortion of the converter currents.

### 3. Proposed control structure

In the case of the above mentioned wind power application, it is crucial to get the most out of the converter, injecting the maximum available reactive power in order to optimize the rating of the converter. An optimized PWM current controller is composed of three main blocks:

- a) *Higher level control loop*: the objective of this control loop is to generate an optimized current reference for the converter taking into account actual grid conditions.
- b) *Current control structure*: the objective of this loop is to obtain good transient and steady-states responses, and therefore it must present appropriate bandwidth characteristics.
- c) *Synchronization*: the purpose of this block is to estimate the voltage grid instantaneous phase in order to generate an optimal current reference.

### a) Higher level control loop: current reference generation

In the considered application, the objective of the converter is to inject the maximum available reactive power in order to minimize voltage drops at the wind farm connection point after a fault clearing. Therefore, the maximum current reference must be defined by the higher control loop.

The direct application of a maximum amplitude current reference at each of the phases may result on a homopolar current injection (in case of phase unbalances at the grid) and if this component is directly removed, the solution may not be optimal from the maximum power injection viewpoint. Thus, the proposed strategy is based on the principle of injecting a higher current in those phases with a higher residual voltage and it is implemented as follows (see Figure 6). The proposed strategy is independent with respect to the nature of the converter output power (active and reactive) and therefore a pure active injection example is presented at this figure, because of simplicity reasons. As it can be seen, the three currents are injected in phase with disturbed grid voltages, injecting the maximum current in the phase with the maximum residual voltage (**a**).

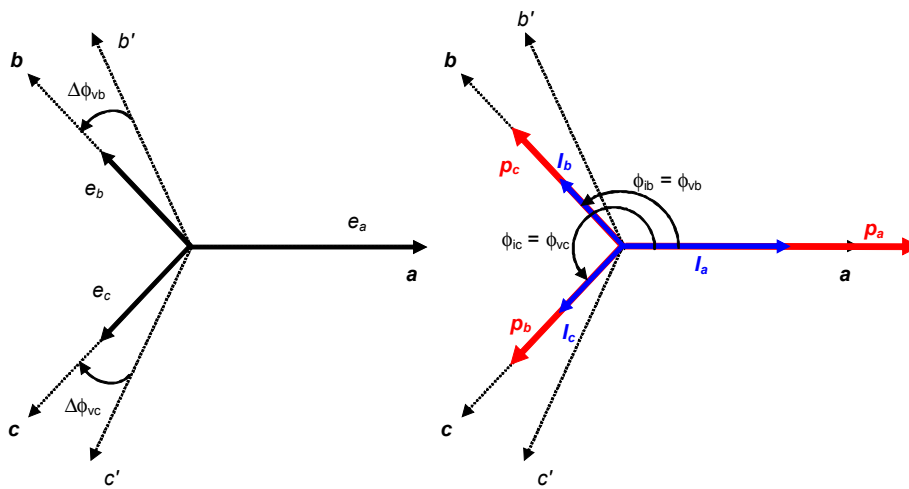


Fig. 6. Maximum power injection for a pure active operation. Grid voltage (left) and injected current and power (right).

- *Current Phase Angle:* The phase angle of each of the phases is derived from the desired power factor:

$$\varphi_{PF} = \tan^{-1}\left(\frac{P_{ref}}{Q_{ref}}\right); \quad \phi_{In} = \phi_{Vn} + \varphi_{PF} \quad (5)$$

- *Current Amplitude:* The sum of the three phase converter currents must be zero (no homopolar sequence) and their amplitudes must be in accordance with residual voltage amplitudes of each of the phases (i.e. the maximum currents must be injected in the phases with the maximum residual voltages as shown in Figure 6). The phases with maximum and minimum residual voltages will be determined by the disturbance characterization module. Supposing for instance that  $E_a = E_{max}$  then  $I_a = I_{max}$ , the amplitude of the other two currents will be calculated as follows in order to guarantee a null zero-sequence current (taking into account the possibility of a phase unbalance), by assuming that the sum of all current components must be zero both in the real and in the imaginary projections:

$$I_b = -I_a \frac{\cos\phi_{ia} \cdot \sin\phi_{ic} - \sin\phi_{ia} \cdot \cos\phi_{ic}}{\cos\phi_{ib} \cdot \sin\phi_{ic} - \sin\phi_{ib} \cdot \cos\phi_{ic}} \quad (6)$$

$$I_c = -\frac{I_a \cdot \sin\phi_{ia} + I_b \cdot \sin\phi_{ib}}{\sin\phi_{ic}}$$

### b) Current control structure

Vector current control structures have been widely proposed for the control of three-phase AC systems because of their good steady-state features (they have a theoretically infinite gain at the rotating frequency and they are thus able to completely eliminate the error at this frequency).

However in the last years a new family of controllers has been introduced as an interesting static alternative to the use of synchronous PI controllers [13], [14], [15] for AC current control applications (both in single and three phase systems): resonant regulators (also known as generalized integrators). These regulators are generally made up of a proportional and an integrator term, which contains a resonant pole aimed at obtaining an infinite gain at the resonance frequency ( $\omega_0$ ):

$$C_R(s) = k_p + \frac{2 \cdot k_i \cdot s}{s^2 + \omega_0^2} \tag{7}$$

This regulator can be easily deduced from the stationary frame equivalent regulator of a synchronous frame PI by building its real equivalent regulator:

$$C_{IG}(s) = k_p + \frac{k_i}{s - j\omega_0} + \frac{k_i}{s + j\omega_0} \tag{8}$$

Thus, the resonant regulator presents a symmetric frequency response and an infinite gain for both positive and negative sequences of the selected frequency. Consequently it is especially well fitted for unbalanced applications like the one considered in this paper. The following figure presents the block diagram of the proposed stationary frame current controller. In addition to the resonant current regulator mentioned before, the system contains a PI for the DC bus voltage control and a zero-sequence component removing function.

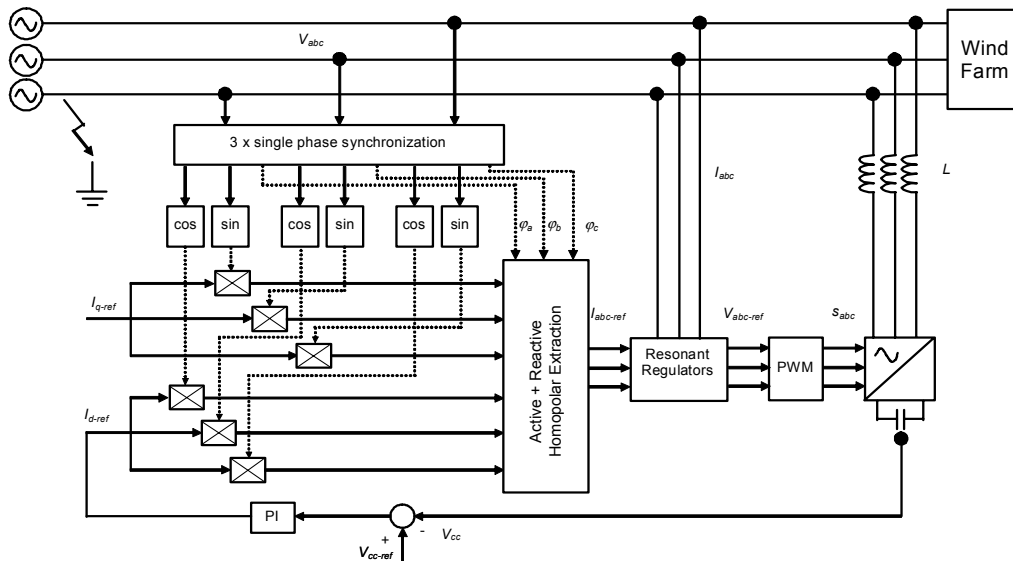


Fig. 7. Proposed improved current control structure.

### c) Synchronization

In order to implement the above presented scalar control structure it is necessary to use single-phase synchronization systems with sufficient dynamics. The dynamics obtained with conventional single-phase synchronization techniques are quite limited (typically between 50 and 100ms) because of the delay introduced by the generation of a virtual three-phase system and the need for eliminating the 100Hz component originated by the phase detector block. Thus, in this paper a real-time DFT (Discrete Fourier Transform) has been used. The implemented real time Expression used to calculate fundamental voltage amplitude and instantaneous phase is for each of the grid phases is:

$$V_1 = \frac{\sqrt{2}}{N} \cdot \sum_{n=0}^{N-1} v(n) \cdot e^{-j \cdot \frac{2\pi n}{N}} \tag{9}$$

### 4. Implementation and Experimental results

The experimental tests have been carried out at a test-bench built at the IKERLAN-IK4 Technological Research Center in Mondragón (Spain). The test-bench (see Figure 8) is basically composed of a voltage source converter connected to a programmable grid (a commercial Profline generator and a zero sequence blocking transformer) through a grid connection inductive filter. The main parameters of the test-bench are presented in Table I.

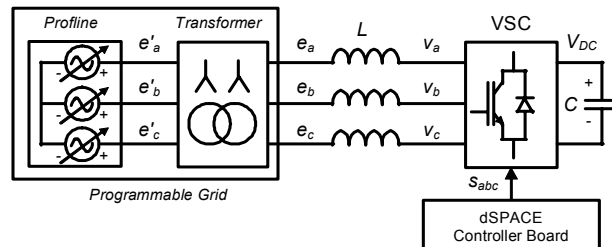


Fig. 8. Scheme of the test-bench used for the experimental improved control strategy validation.

This test-bench permits to validate the transient reactive power injection capability of the proposed STATCOM control structure, which as it has been shown in the literature may be crucial for the grid response improvement of fixed speed wind farms [8]. A “D Type” voltage sag has been considered (according to [12]), comparing the obtained experimental results with simulation results (obtained with Matlab/Simulink).

TABLE I. Main Parameters of the Experimental Test-Bench

| Symbol    | Magnitude                         | Value         |
|-----------|-----------------------------------|---------------|
| $V_{DC}$  | DC bus voltage                    | 400V          |
| $C$       | DC bus capacitor                  | 235 $\mu$ F   |
| $L$       | Grid connection filter inductance | 3mH           |
| $r$       | Grid connection filter resistance | 200m $\Omega$ |
| $f_s$     | Sampling Frequency                | 5kHz          |
| $f_{sw}$  | Switching Frequency               | 5kHz          |
| $E$       | Transformer secondary voltage     | 220 $V_{LL}$  |
| $E'$      | Transformer primary voltage       | 380 $V_{LL}$  |
| $I_{NOM}$ | Converter nominal current         | 15A           |

Experimental and simulation results are presented in Figures 9-13. As it can be observed, the control structure permits to optimize the injected reactive power by injecting a higher current in the phases with higher residual voltages, with relatively smooth current transients (Figures 10 and 11). Before the disturbance the converter is absorbing reactive power, but once the disturbance started it changes rapidly its operation mode in order to generate the maximum available reactive power (Figure 12). Finally, Figure 13 shows how DC bus voltage oscillations increase during the transient due to the converter three phase power unbalance (which is necessary to optimize the amount of injected power).

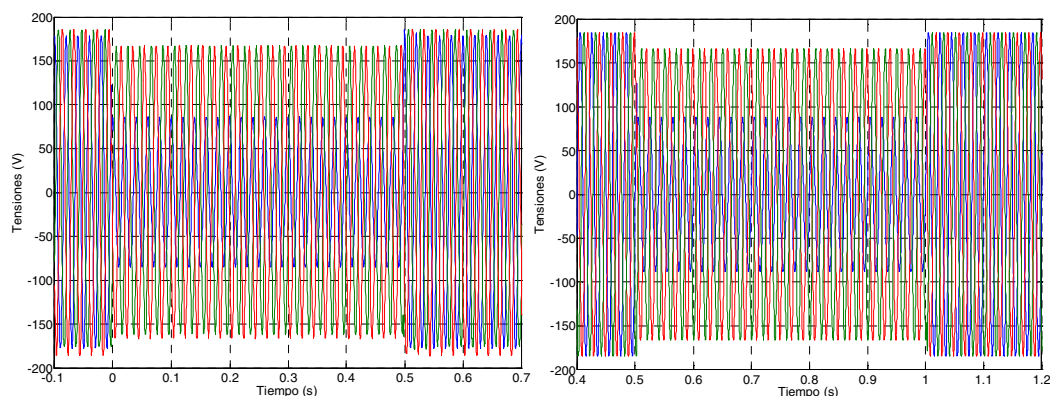


Fig. 9. Voltage at the converter connection point. Experimental (left) and simulation (right).

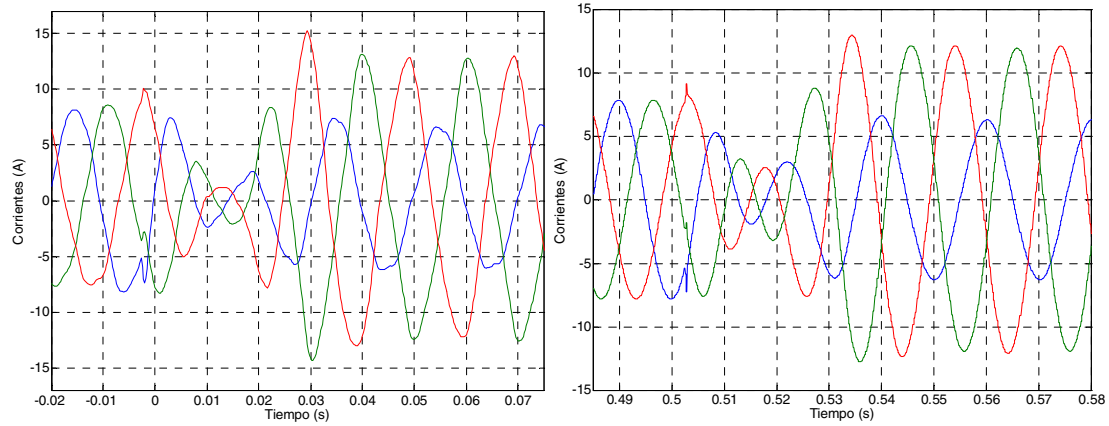


Fig. 10. Converter current at the disturbance beginning. Experimental (left) and simulation (right).

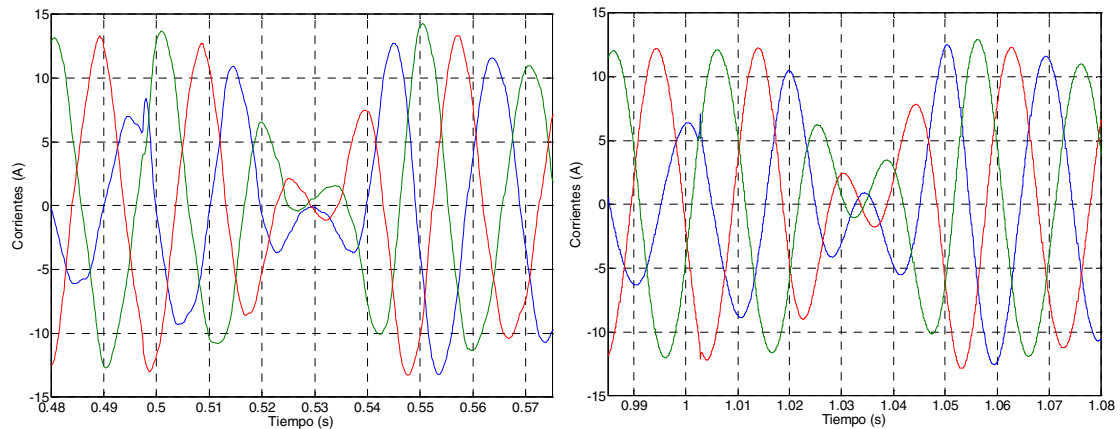


Fig. 11. Converter current at the disturbance end. Experimental (left) and simulation (right).

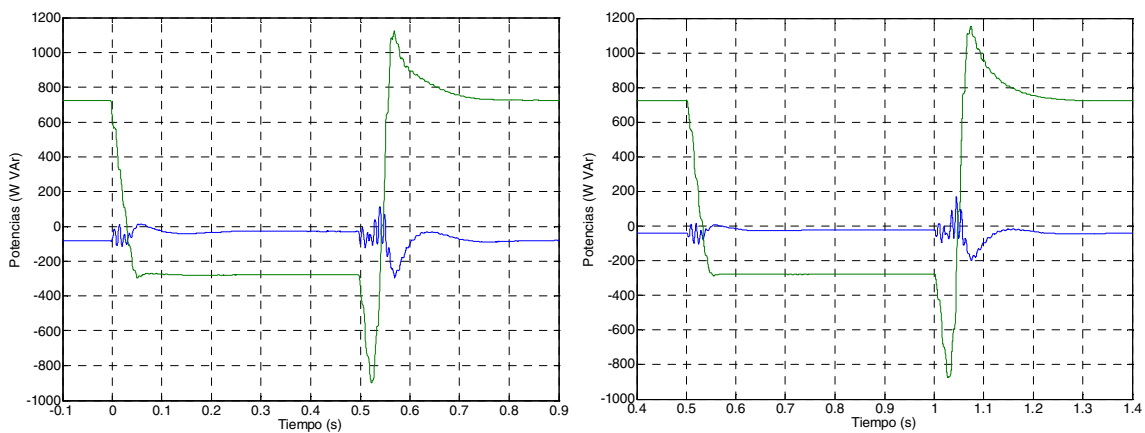


Fig. 12. Converter active and reactive power (one phase). Experimental (left) and simulation (right).

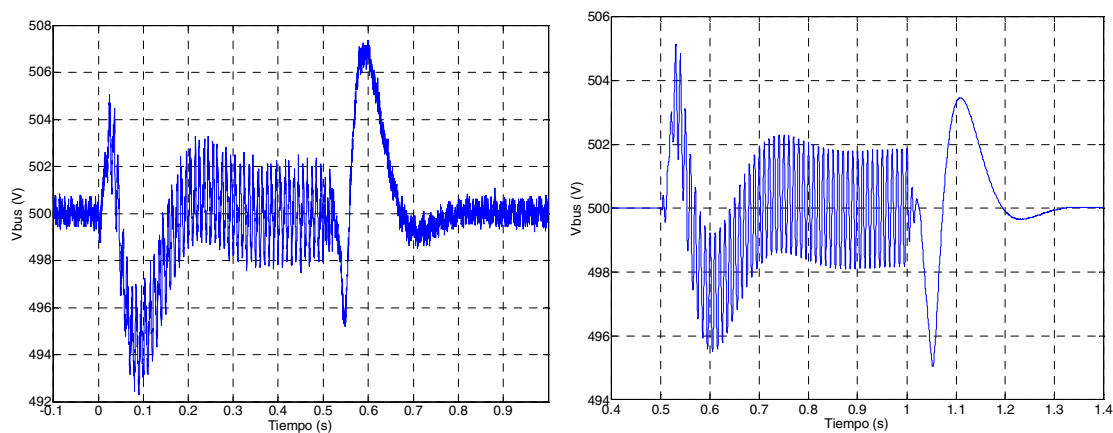


Fig. 13. Converter DC bus voltage. Experimental (left) and simulation (right).

## 5. Conclusion

This paper presents an optimized STATCOM control for wind power applications. The main features of this control are:

- The use of 3 single-phase synchronization functions in order to deal not only with amplitude unbalances but also with phase unbalances.
- The use of 3 single-phase controllers based on resonant regulators.
- Separated generation of active and reactive references which are then adjusted in order to obtain a current reference without zero-sequence component.

The proposed structure has been validated experimentally and in simulation, using a reduced scale STATCOM prototype, showing that it is well adapted for the concerned application.

## 6. References

- [1] Saad-Saoud Z, Lisboa M, Ekanayake J, Jenkins N, Strbac G. The application of STATCOMS to wind farms. IEE Proceedings Generation Transmission and Distribution, Vol. 145, No 5, Sep.1998, pp 511-516.
- [2] K. H. Sobrink, N. Jenkins, F. C. A. Schettler, J. Pedersen, K. O. H. Pedersen, and K. Bergmann, "Reactive power compensation of a 24 MW wind farm using a 12-pulse voltage source converter," in Proc. CIGRÉ Int. Conf. Large High Voltage Electric Systems, 1998.
- [3] Improvement of Wind Farm Output Power Quality Using Advanced Static VAr Compensators Non-Nuclear Energy – R&D Component (JOULE III), 1996–1998, Project Reference: JOR3950091.
- [4] Aten M, Martinez J, Cartwright P.J. Fault Recovery of a Wind farm with Fixed-Speed Induction Generators using a STATCOM. Wind Engineering, Vol. 29, No. 4, 2005.
- [5] Xueguang W, Atputharajah A, Changjiang Z, Jenkins N. Application of a Static Reactive Power Compensator (STATCOM) and a Dynamic Braking Resistor (DBR) for the Stability Enhancement of a Large Wind Farm. Wind Engineering, Vol. 27, No. 2, 2003.
- [6] W. Freitas, A. Morelato, W. Xu, and F. Sato, "Impacts of ac generators and DSTATCOM devices on the dynamic performance of distribution systems," IEEE Trans. Power Delivery, vol. 20, no. 2, pp. 1493–1501, Apr. 2005.
- [7] C. Chompoo-inwai, C. Yingvivanapong, K. Methaprayoon, and W. J. Lee, "Reactive compensation techniques to improve the ride-through capability of wind turbine during disturbance," IEEE Trans. Ind. Applicat., vol. 41, pp. 666–672, May-Jun. 2005.
- [8] H. Gaztañaga, I. Etxeberria-Otadui, D. Ocnasu and S. Bacha, "Real-Time Analysis of the Transient Response Improvement of Fixed-Speed Wind Farms by Using a Reduced-Scale STATCOM Prototype". IEEE Transactions on Power Systems, Vol. 22, No. 2, May 2007.
- [9] PO 12.3. Voltage Sag Response Requirements of Wind Power Facilities, Operation Procedure (in Spanish) Spanish System Operator (REE), 2006.
- [10] R. Grünbaum, P. Halvarsson, D. Larsson, and P. R. Jones, "Conditioning of power grids serving offshore wind farms based on asynchronous generators," in Proc. IEE PEMD 2004, 2nd Int. Conf. Power Electronics, Machines and Drives, Edinburgh, U.K., 2004.
- [11] H. Gaztañaga, I. Etxeberria-Otadui, S. Bacha, D. Roye, "Fixed-Speed Wind Farm Operation Improvement by Using DVR Devices" IEEE ISIE'07, 2007, Vigo, Spain.
- [12] M. H.J. Bollen, "Understanding Power Quality Problems. Voltage Sags and Interruptions", IEEE Press Series on Power Engineering, ISBN 0-7803-4713-7, 2000.
- [13] M. Bojrup, P. Karlsson, M. Alakulla, and L. Gertmar, "A multiple rotating integrator controller for active filters," in Proc. EPE Conf., Lausanne, Switzerland, 1999, CD-ROM.
- [14] X. Yuan, J. Allmeling, W. Merk, and H. Stemmler, "Stationary frame generalized integrators for current control of active power filters with zero steady state error for current harmonics of concern under unbalanced and distorted operation conditions," in Proc. IEEE-IAS Annu. Meeting, Conf. Rec., Roma, Italy, 2000, pp. 2143–2150.
- [15] I. Etxeberria-Otadui, U. Viscarret, M. Caballero, A. Rufer and S. Bacha, "New Optimized PWM VSC Control Structures and Strategies Under Unbalanced Voltage Transients", IEEE Transactions on Industrial Electronics. Accepted in May 2007, waiting for publication.